Development of a Simulation-Based Model for Accuracy Analysis of Optical Rotary Encoders Under Mechanical Vibrations

Violeta Krcheva
Laboratory Assistant
Goce Delcev University, Stip
Faculty of Mechanical Engineering
Republic of North Macedonia

PhD Student
University „St. Kliment Ohridski"
Faculty of Technical Sciences – Bitola
Republic of North Macedonia

Stojance Nusev
Professor
University „St. Kliment Ohridski"
Faculty of Technical Sciences - Bitola
Republic of North Macedonia

Miša Tomić
Assistant
University of Nis
Faculty of Mechanical Engineering - Niš
Serbia

This study presents the development of an innovative simulation-based model for analysing the accuracy of optical rotary encoders subjected to mechanical vibrations. The proposed approach establishes a digitally controlled environment that emulates real operational conditions, enabling systematic examination of dynamic effects on encoder performance. The model integrates essential components that allow the formation of a system capable of operating both within a digital simulation environment and under real experimental conditions with controlled generation of mechanical vibrations. By simulating diverse operating scenarios, the model provides detailed characterisation of measurement deviations and identifies variations in measurement error of the investigated encoder as a function of changes in input parameters. The resulting insights support predictive evaluation of measurement error behaviour and enable systematic assessment of encoder accuracy under varying vibration and operating conditions. Consequently, the proposed simulation method offers a reliable and reproducible tool for investigating vibration-induced measurement errors in advanced precision systems.

Keywords: *SolidWorks, CAD Model, MATLAB & Simulink, Block Diagram, Vibration Parameters, Rotational Speed.*

1. INTRODUCTION

The sustained progression of digital technologies and information-driven engineering has facilitated substan–tial enhancements in precision, control, and automation within technical systems and industrial operations. Within this context, optical encoders function as high-fidelity electromechanical sensors, extensively deployed in modern automation, control, and metrological applications. Depending on functional requirements, optical encoders are generally classified as linear or rotary. Linear encoders measure translational displa–cement, whereas rotary encoders (Fig. 1) are designed for the assessment of angular position and rotational movement [1–3].

Figure 1. An optical rotary encoder [4]

The operating principle of a rotary optical encoder relies on the modulation of a light beam by a rotating disc engineered with alternating regions of contrasting optical characteristics, such as transparent and opaque or reflective and non-reflective sectors (Fig. 2). This disc is rigidly coupled to the shaft of the monitored element, ensuring synchronous rotation and enabling continuous real-time tracking of angular position [5,6].

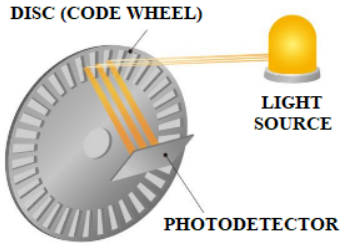

Figure 2. The fundamental functional principle of an optical rotary encoder [4]

In a conventional arrangement, a light source (typi–cally a light-emitting diode) projects a focused beam that interacts with the patterned disc, either through transmission or reflection. As the disc rotates, the pattern modulates the light, generating a sequence of pulses. These variations are detected by photosensitive elements such as photodiodes or phototransistors situ–ated opposite the light source. Each light transition produces a discrete electrical pulse; the series of pulses, defined by frequency, phase, and sequence, allows precise determination of angular position, rotational direction, and velocity [7,8].

A key determinant of measurement fidelity is the number of lines or windows on the coding disc. Higher line density generates more pulses per rotation, thereby

Received: January 2026, Accepted: February 2026
Correspondence to: Violeta Krcheva
Faculty of Mechanical Engineering,
Krste Misirkov No. 10-A, Stip 2000, RNM
E-mail: violeta.krceva@ugd.edu.mk
doi: 10.5937/fme2602214K

enhancing resolution. Each window provides a distinct optical path, which the sensor converts into an electrical signal. Encoders are available in a range of resolutions, commonly 100, 200, 360, 500, or 1000 pulses per revolution (PPR), allowing selection according to the desired accuracy [9–11].

Sustaining high precision under operational conditions necessitates that rotary encoders possess resilience against dynamic disturbances, among which mechanical vibrations are most pervasive. Such oscillations typically arise in automated systems, during positioning tasks, or as a consequence of rapid changes in drive and control regimes, imposing dynamic loads that mirror practical industrial scenarios [12–14].

Accurate evaluation of encoder performance under dynamic conditions requires rigorous investigation of vibrational effects. Contemporary sensor metrology increasingly relies on methodologies capable of simulating such disturbances within controlled environments. Characteristic vibration parameters: frequency, amplitude, and exposure duration (Fig. 3), are systematically varied to quantify their impact on measurement integrity [15,16].

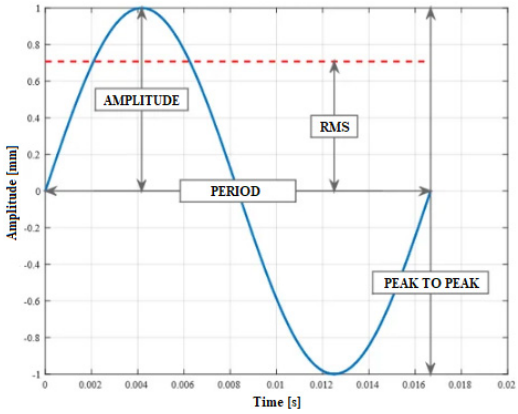

Figure 3. Mechanical vibration parameters [17]

Vibration frequency (Hz) influences the sensor's dynamic response, as different ranges may induce diverse signal distortions, from low-frequency drifts affecting long-term stability to high-frequency oscillations introducing noise or false triggering. Optical encoders, due to their temporal sensitivity, display pronounced responsiveness across low (<10 Hz), medium (10–100 Hz), and high (>100 Hz) frequency ranges. Vibration amplitude (mm or μm) represents the intensity of mechanical oscillations. Even micrometre-scale displacements, particularly at elevated rotational speeds, can result in phase shifts, signal edge distortions, or loss of discrete logical states within the output. The duration of exposure (s) exerts a cumulative influence on measurement reliability. Extended vibrational action may not only lead to progressive measurement errors but also trigger thermomechanical effects or structural displacements that impact optical interactions and sensor alignment [18–20].

2. REVIEW OF LITERATURE

This section synthesises contemporary research investigating the effects of mechanical vibrations on the metrological performance of optical encoders. Alejandre and Artés [21] identified that encoder functionality is predominantly influenced by structural deformations, thermal fluctuations, and vibrational disturbances within the mechanical system. While extensive analyses have addressed thermal and deformation effects, comparatively fewer investigations have systematically explored the response of optical encoders under dynamic vibrational loads. In their subsequent study, Alejandre and Artés [22] extended the evaluation to include vibrational influence, offering quantitative assessment and classification of oscillatory effects, thereby elucidating operational limitations in diverse technical and industrial settings.

Historically, investigations into positioning errors in CNC metal-cutting machinery have concentrated on the structural characteristics of the machine rather than the encoder. Weck et al. [23], respectively Florussen et al. [24] introduced methodologies for evaluating geometric inaccuracies in multi-axis CNC systems via three-dimensional volumetric measurements, culminating in a generalised error model applicable across varied machine configurations. These approaches facilitated software-based compensation and enabled precise diagnosis of functional deviations. The studies highlighted that meticulous design of the measurement system and accurate error modelling, based on correlating parameters affecting precision, are indispensable for reliable diagnostics.

Although synchronisation errors in mobile components are frequently attributed to machine architecture, emerging evidence suggests that encoders themselves constitute a non-negligible source of measurement deviation. Resor et al. [25] applied a digital time-interval technique to quantify torsional vibrations in rotating shafts, incorporating a calibration procedure that generated reference sequences matching true angular intervals. A resampling algorithm ensured equidistant temporal samples, mitigating frequency blurring caused by rotational variability, even for high-precision optical encoders.

Further innovations aimed at mechanical isolation of encoders were proposed in patents by Shiro [26] and Shinichi [27], utilising flexible couplings, sliders, and auxiliary structures to attenuate vibrational influence. Nonetheless, literature surveys indicate that systematic characterisation of encoder performance across operational frequency ranges under dynamic conditions remains limited.

Alejandre and Artés [28] confirmed that optical encoders generally retain high accuracy under vibrational excitation, although deviations are often misattributed to CNC components such as gears or belts. They emphasised the necessity of models explicitly evaluating encoder performance under vibrational regimes. Their approach introduced the concept of "measurement error within a frequency range", moving beyond resonance identification and signal acceleration, thereby providing a more comprehensive assessment of operational performance. The model considered both error magnitudes at resonance and across non-resonant frequencies, with critical factors including signal type, non-linear variations, sampling rate, and signal compo–

sition—parameters essential for accurate performance evaluation under dynamic conditions.

Experimental application of this framework yielded high-resolution spectra, revealing multiple instability zones within the analysed frequency domain. Tests adhered to EN 60068-2-6:1996 [29], exposing encoders to variable frequencies, with amplitudes tailored to commercial specifications. Recorded measurement deviations reached up to threefold the nominal accuracy, illustrating that optical encoders may act as substantial error sources under high-frequency vibrational exposure, despite compliance with international environmental standards. These findings provide actionable insights for both designers and users, facilitating optimisation of encoder configurations and operational strategies.

López et al. [30] extended the analysis to three commercially available optical linear encoders under various mounting conditions, quantifying the effect of vibrational directionality and position on measurement accuracy. Test protocols, conducted in accordance with EN 60068-2-6 [29], specified frequency ranges, amplitudes, and exposure durations. Results highlighted that errors frequently exceeded nominal specifications, particularly where mounting positions induced additional resonances, emphasising the importance of installation conditions in metrological reliability.

While linear encoders have been examined extensively, systematic investigations of optical rotary encoders under vibrational influence have remained sparse. Addressing this gap, Krcheva et al. [31] developed an experimental framework for evaluating rotational encoder accuracy under controlled vibrational conditions. Their methodology encompassed three commercial encoders of differing resolutions (100 PPR, 360 PPR, and 1000 PPR), exposing them to precisely defined vibration parameters—frequency, amplitude, and duration. Reference signals enabled quantification of output deviations and identification of sensitive frequency bands. Comparative analysis revealed that encoder resolution directly influenced signal stability and resistance to dynamic perturbations, informing both practical deployment and selection of encoder types for vibration-prone environments. MATLAB-based data processing facilitated detailed evaluation, encompassing component configuration, result analysis, and graphical visualisation of performance. The findings underscored that high-resolution encoders are indispensable for high-accuracy applications, whereas lower-resolution devices may be adequate in environments with limited vibrational impact.

2.1 Limitations of Existing Literature and Motivation for a Simulation-Based Approach

Despite several experimental studies, a notable research void persists in the development of predictive, simulation-orientated models for optical rotary encoders under vibrational influence. Current literature largely relies on empirical testing, which constrains rapid and cost-efficient evaluation of diverse operating scenarios and parameter variations. Such reliance necessitates full-scale experimental setups for each condition, posing significant logistical and temporal challenges.

Accordingly, the development of a simulation-based framework is imperative. Such a model would enable reproducible prediction of measurement errors, sensitivity analysis under varying dynamic conditions, and virtual experimentation to identify critical parameters. This approach would substantially reduce the need for repeated physical testing, providing a robust tool for engineers and researchers to optimise encoder performance and develop strategies to minimise measurement errors in a virtual environment prior to real-world implementation.

3. MODEL DESIGN AND DEVELOPMENT

3.1 Graphical Design of the Mechanical System

During the preliminary design stage, a schematic representation of the integrated mechanical system was developed, comprising the drive unit, transmission assembly, and the optical rotary encoder under investigation, with each component assigned a distinct functional role within the system's overall dynamic behaviour. At this conceptual phase, the framework was designed to enable controlled and isolated application of mechanical vibrations to the encoder while maintaining the stability and reference characteristics of the remaining components (Fig. 4).

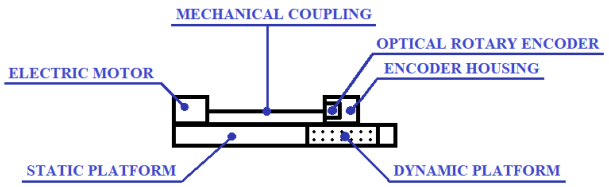

Figure 4. Design of the system

The drive unit was represented by an electric motor, serving as an idealised reference source of rotational motion and assumed to operate under perfectly stable and predictable conditions. Mechanical disturbances were neglected, and the degrees of freedom were strictly constrained, thereby establishing an invariant angular reference for subsequent comparative analyses within the simulation environment.

The transmission interface, realised through a mechanical coupling between the drive unit and the encoder, was conceptualised as a rigid and lossless system, devoid of elastic deformation or geometric misalignment. Within this framework, torque was transmitted with complete fidelity, ensuring that any observed deviations in angular position originated exclusively from vibrational effects acting on the encoder.

The encoder was treated as a mechanically sensitive element and was mounted on a dynamic platform engineered to introduce controlled and localised vibrations. This configuration ensured that oscillatory loads were applied solely to the encoder, while the remainder of the system maintained structural stability.

The operational principle of the simulation was founded on a comparative measurement approach, whereby the angular position of the encoder under test was monitored relative to the reference provided by the drive

unit. For this purpose, the electric motor incorporated a high-resolution encoder, which provided reliable and reproducible reference data for subsequent error quantification.

Dynamic excitations, in the form of mechanical vibrations, were expected to induce measurable deviations in the encoder output. Accordingly, the simulation framework was designed to detect and quantify these deviations, correlate them with the imposed vibration parameters, and evaluate their impact using appropriate numerical metrics.

The outcome of this phase was the establishment of a coherent structural and functional framework, delineating the interaction logic between the system components and providing a systematic foundation for the subsequent development of the CAD model.

3.2 Development of the CAD Model

Based on the conceptual framework, a detailed three-dimensional CAD model was developed in SolidWorks (version 2022–2023), in which the principal geometry, structural configuration, and spatial arrangement of the components were specified in accordance with the established design logic (Fig. 4).

The electric motor was positioned on the left-hand side of the assembly and was modelled as the source of rotational motion with a stable shaft (Fig. 5). Its attachment to the static platform was constrained to ensure mechanical stability and reproducibility of motion within the CAD model.

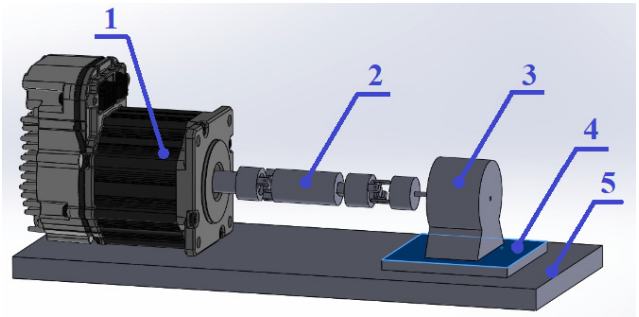

Figure 5. CAD model of the system: 1 – Electric motor; 2 – Mechanical coupling; 3 – Encoder housing; 4 – Dynamic platform; 5 – Static platform

Torque transmission between the motor and the encoder was realised via a mechanically aligned transmission mechanism, designed to preserve coaxial alignment and ensure reliable kinematic connectivity between the connected components.

The optical rotary encoder was located on the right-hand side and was enclosed within a precisely modelled housing (Fig. 6). Kinematic constraints were applied to both the housing and shaft to secure accurate alignment with the drive shaft, thereby guaranteeing mechanical integration and stability within the system.

A critical structural feature was the dynamic platform supporting the encoder, highlighted by the blue upper surface in Fig. 5. This platform functioned as a localised mechanical base for introducing controlled vibrations, ensuring that oscillatory effects were confined to the encoder and its housing, without affecting the remaining system components.

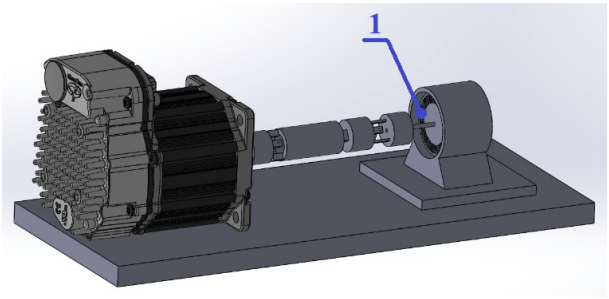

Figure 6. Optical rotary encoder position (1)

The resulting CAD model generated a core geometric and structural representation, providing the structural basis for its subsequent integration into MATLAB & Simulink.

3.3 Importing the CAD Model into MATLAB & Simulink

Transferring the CAD representation of the mechanical assembly from SolidWorks into MATLAB & Simulink constitutes an essential step in the simulation workflow, as it converts the three-dimensional structural model into a functionally organised block-diagram framework. The CAD assembly was exported using the Simscape Multibody Link plugin, which generated an XML file containing the geometric configuration, mass properties, joint definitions, and dynamic parameters of the individual components. This XML-based representation was subsequently imported into MATLAB & Simulink, where the physical structure was automatically translated into an interconnected multibody model. This process required the systematic mapping of kinematic linkages, mechanical constraints, and component interactions into corresponding mathematical and logical blocks within the simulation environment.

The imported CAD model functions as a structural reference, defining spatial arrangement, orientations, kinematic couplings, and mechanical constraints (fixed, coaxial, concentric, or mobile). Essential data—including geometry, mass properties, coordinate positions, and constraint definitions—are extracted and mapped to the system's degrees of freedom, forming the structural basis for the functional simulation.

A key aspect is component abstraction. While SolidWorks maintains full geometric fidelity, MATLAB & Simulink represent components based on functional roles. The electric motor is abstracted as a rotational source block with a defined reference axis for connected components. Couplings and intermediary mechanisms are represented as transmission blocks, incorporating compliance or constraint parameters. The optical rotary encoder, originally a mechanical element, is represented as a sensor block interfacing with signal-processing blocks to convert angular position into digital output for analysis.

Subsidiary components are parameterised as discrete blocks capable of receiving external inputs. Motions that are mechanically feasible in the CAD model are transformed into controllable input signals, enabling parameterised experimentation and maintaining a direct relationship between geometric configuration and functional behaviour.

Mechanical linkages are interpreted as causal and functional connections within the block diagram. Coor–dinate systems and spatial relationships are converted into signal variables, prioritising information flow and dynamic response over physical form. Simscape Multi–body enables direct conversion of CAD assemblies into block-diagram format, preserving bodies, joints, and reference frames while supporting hierarchical organi–sation, parameterisation, and systematic evaluation.

The functional model interfaces with control and signal-processing blocks, allowing dynamic manipula–tion of inputs such as rotational speed and real-time acquisition of encoder signals. The block diagram does not replicate CAD geometry visually but establishes a functionally coherent system consistent with the mecha–nical logic defined in SolidWorks.

This approach enables the import of the CAD model as a preliminary step towards generating the final block diagram, representing the complete system model and facilitating subsequent simulations.

3.4 Structure and Function of the Block Diagram

The simulation model implemented in MATLAB & Simulink (R2023a) represented a direct functional extension of the CAD model developed in SolidWorks, whereby the system's spatial and structural logic was transformed into a dynamic simulation framework organised through a block-diagram architecture. The model was configured to enable the parallel generation of two angular trajectories: a reference angular position serving as an idealised kinematic benchmark, and a measured angular position resulting from the physical transmission system and the measurement process under realistic constraints and disturbances. This approach established a clear and direct relationship between the prescribed input parameters and the resulting deviations, extending the simulation beyond purely visual signal inspection to include quantitative results displayed directly within the block-diagram environment. For improved clarity and structural transparency, the complete block-diagram architecture is presented in two complementary segments (Fig. 7a and Fig. 7b).

The input parameters were positioned on the left-hand side of the diagram and were organised to allow explicit specification of the fundamental operating conditions. Within the MOTOR SPEED INPUT (RPM) section, the rotational speed was defined via the *Motor_Speed_Command* block, which provided a constant speed value expressed in RPM (Fig. 8). To ensure compatibility with the remainder of the model, the signal was passed to the *RPM_to_RadPerSec* block, where it was converted into angular velocity in rad/s. Subsequent signal conditioning was performed by the *Motor_Speed_Signal_Product* block, which prepared the signal for integration with the time axis and the mechanical subsystem.

The temporal component of the simulation was defined within the SIMULATION TIME INPUT (s) section, where the simulation duration was specified using the *Simulation_Time* block (Fig. 9). Within this part of the model, the fundamental kinematic relati–onship for generating the reference angular position was established through the *Angular_Displacement_Com–putation* block. The resulting signal represented a stable and idealised reference angular trajectory, serving as the basis for subsequent comparison with the measured angular position obtained from the mechanical and measurement subsystems.

In parallel with the kinematic reference branch, a dedicated structure for mechanical vibration generation was implemented in the lower-left section of the block diagram. The frequency parameter was specified via the *Vibration_Frequency_Command* block (Fig. 10) within the VIBRATION FREQUENCY INPUT (Hz) section, after which it was converted to angular frequency using the *Hz_to_RadPerSec* block. The frequency argument was prepared in the *Angular_Frequency_Computation* block, while the resulting time-dependent oscillation was generated through the *Vibration_Excitation_Signal* block.

The vibration amplitude was defined independently via the *Vibration_Amplitude_Command* block (Fig. 11), located within the VIBRATION AMPLITUDE INPUT (mm) section. The linear displacement representing the physical vibrational excitation of the system was obtained by combining the prescribed amplitude with the sinusoidal signal in the *Vibration_Displacement_Product* block. This configuration enabled clear, modular, and precise control of the two key vibration parameters—frequency and amplitude—thereby ensur–ing stable and reproducible conditions for simulation-based analysis.

The central section of the block diagram corres–ponded to the physical representation of the mechanical system and was implemented through blocks identified by the prefixes *MECH_* and *JNT_*. This segment constituted a simulation analogue of the real mechanical transmission, in which rotational motion was modelled as a mechanical interaction between interconnected bodies. Spatial orientation and the coordinate reference frame were defined by the *REF_WorldFrame* block, while the connection to the system's base structure was established via *TF_BaseToWorld* and *MECH_Base Frame*. In this way, a well-defined geometric frame–work was established, within which all subsequent rotations and displacements were interpreted in a consistent and physically meaningful manner.

The drive section of the system was modelled by the *MECH_Motor* block, which generated rotational motion. This motion was transmitted through the revolute joint *JNT_Revolute_MotorOutput* and propa–gated along the mechanical axis *MECH_MotorShaft*. Further transmission towards the Cardan section was achieved via *MECH_DriveShaft_ToCardan* and the *DriveShaft_ToCardan* interface, ensuring that the rotation followed a physically defined pathway relevant for the analysis of dynamic effects. The Cardan structure was modelled as a system of revolute joints and mechanical cross elements, with the input rotation defined via *JNT_Revolute_CardanInput*. The first Cardan element was implemented using *MECH_CardanCross_1*, while the output rotation was trans–mitted through *JNT_Revolute_CardanOutput* to *MECH_IntermediateShaft*. Further transmission was realised through the second Cardan segment, compri–

sing *MECH_CardanCross_2* and *JNT_Revolute_ Car–danIntermediate*. This configuration enabled an accurate representation of the kinematic relationships and their sensitivity to mechanical vibration exposure.

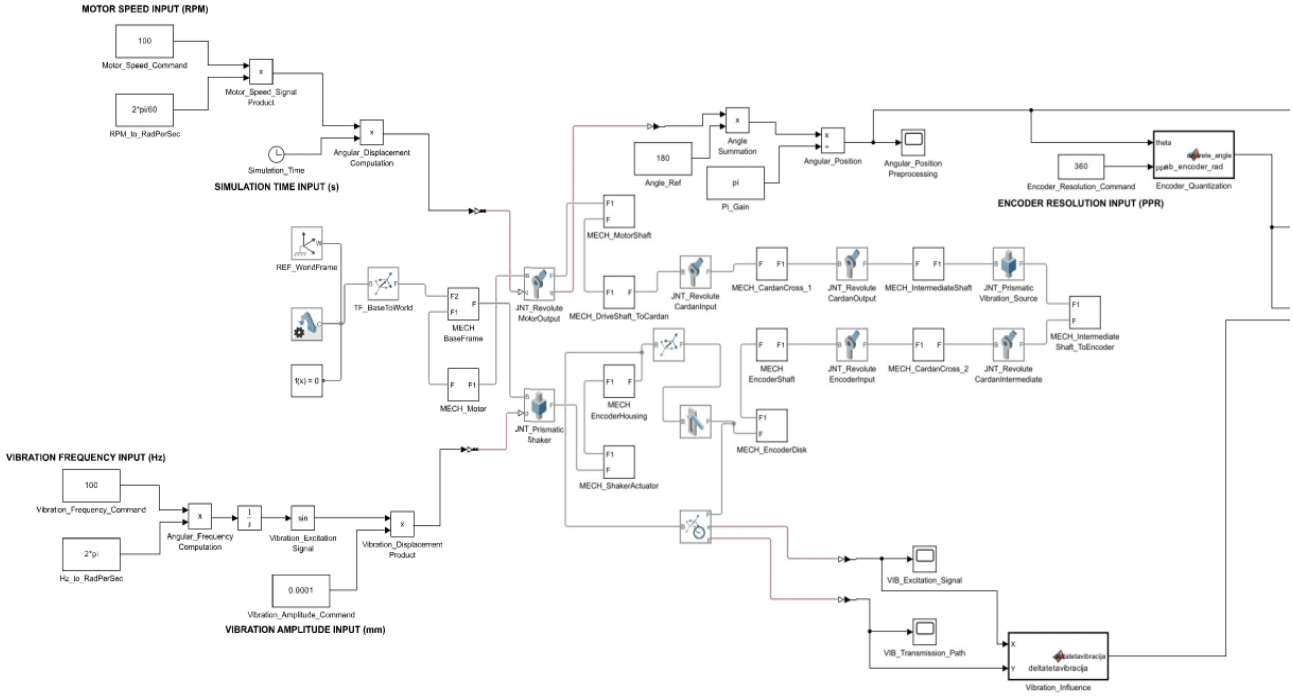

a)

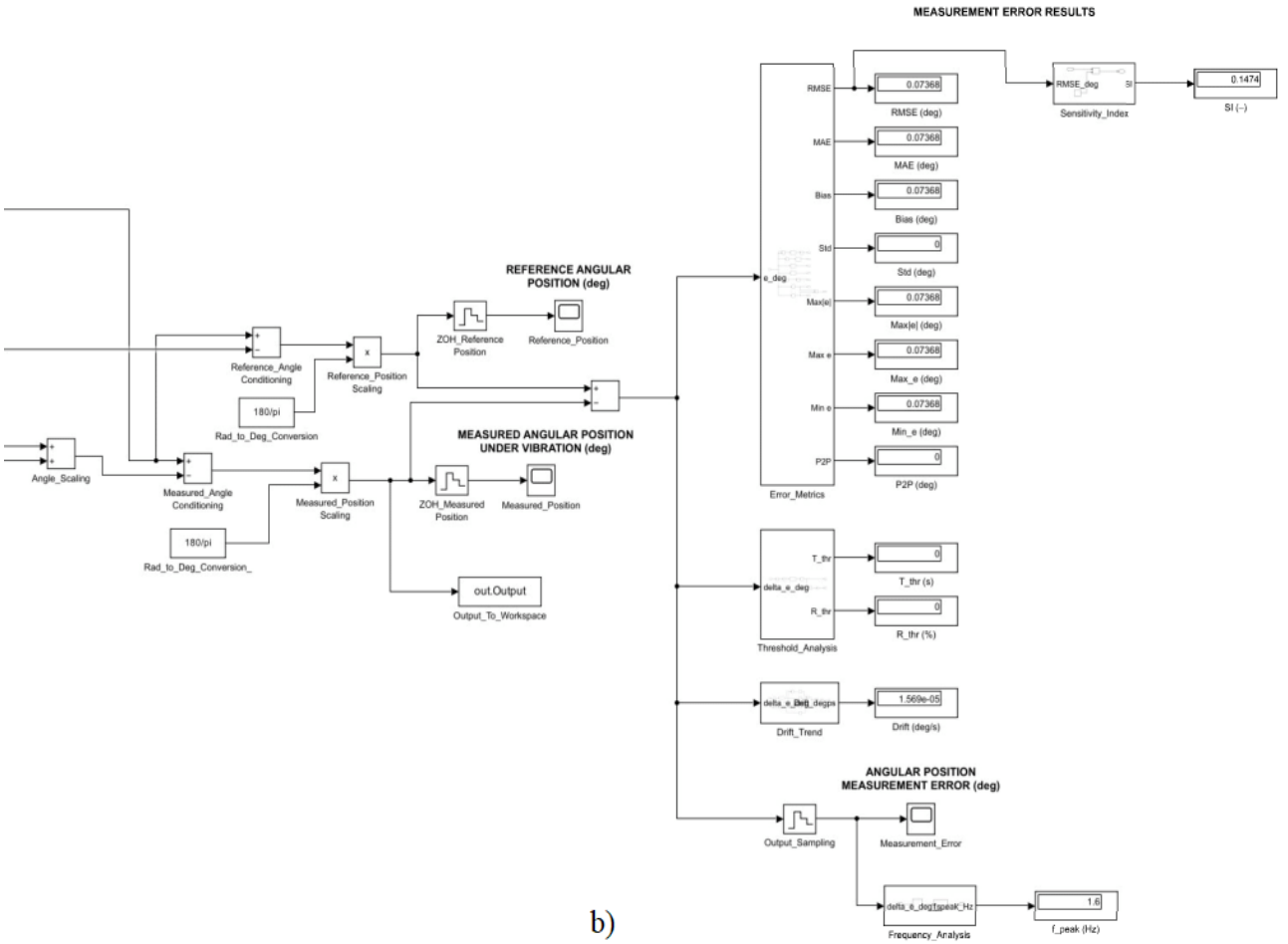

b)

Figure 7. Block diagram of the simulation model: a) Left segment of the model; b) Right segment of the model

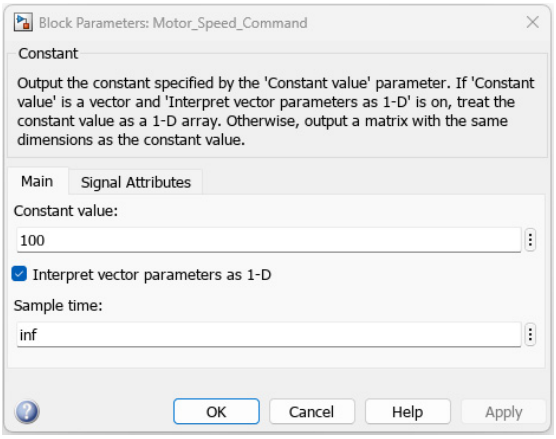

Figure 8. Motor_Speed_Command block window

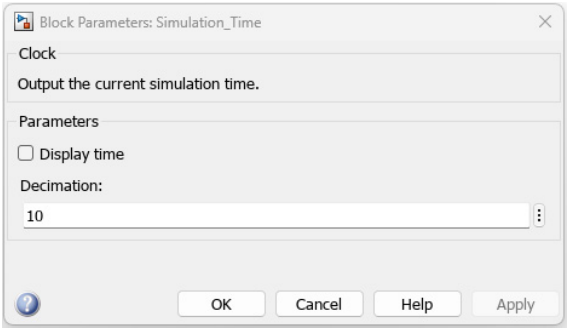

Figure 9. Simulation_Time block window

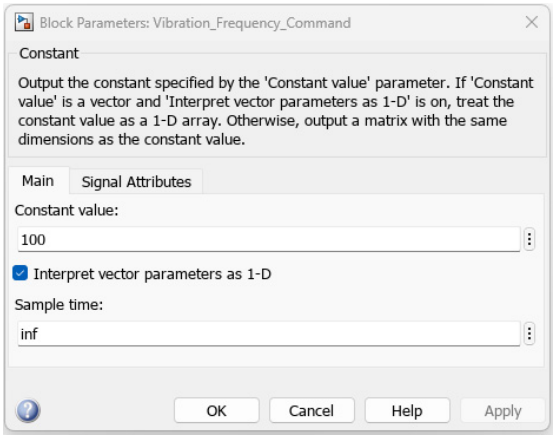

Figure 10. Vibration_Frequency_Command block window

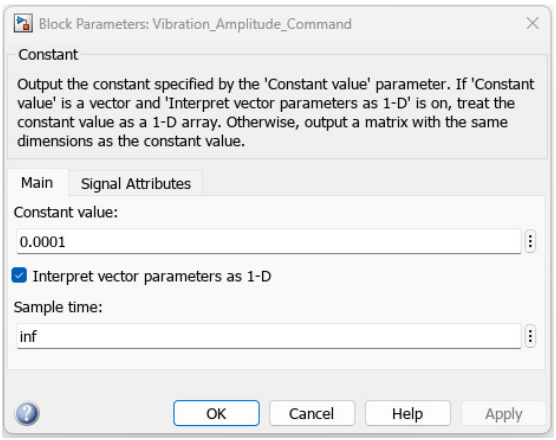

Figure 11. Vibration_Amplitude_Command block window

Vibrations within the mechanical system were realised through prismatic elements enabling linear oscillatory motion. The actuation function was implemented using *JNT_Prismatic_Shaker* and *MECH_ShakerActuator*, while the point of vibration input was defined by *JNT_Prismatic_Vibration_Source*. Through the mechanical connection *MECH_IntermediateShaft_To Encoder*, the vibrational effect was transmitted to the encoder, whereby the disturbance acted as a real physical quantity rather than an artificially introduced signal.

The mechanical structure of the encoder was composed of *JNT_Revolute_EncoderInput*, *MECH_EncoderShaft*, *MECH_EncoderDisk*, and *MECH_EncoderHousing*. This configuration clearly distinguished the rotational element carrying the measurement information from the static component serving as the reference and supporting structure. Such a separation enabled a more realistic interpretation of relative motion and potential micro-displacements induced by mechanical vibrations.

In the upper central segment, the reference angular component was generated using the parameters defined by *Angle_Ref* and *PI_Gain*, which enabled the specification of the initial angle and precise angular conversions. The combination of angular components was realised through *Angle_Summation*, yielding the *Angular_Position* signal. Prior to its use as a measurement quantity, the signal was subjected to additional processing within *Angular_Position_Preprocessing*, thereby ensuring signal stability and structural consistency.

The encoder resolution was specified via the *Encoder_Resolution_Command* block (Fig. 12) within the ENCODER RESOLUTION INPUT (PPR) section, thereby defining the discrete nature of the measurement process. Quantisation of the angular signal was performed in the *Encoder_Quantization* block, whose output *qpab_encoder_angle_rad* represented the quantised angular position. This step modelled a fundamental characteristic of optical encoders, namely that angular position is not measured continuously but through discrete pulses, which directly affects the accuracy and sensitivity of the system.

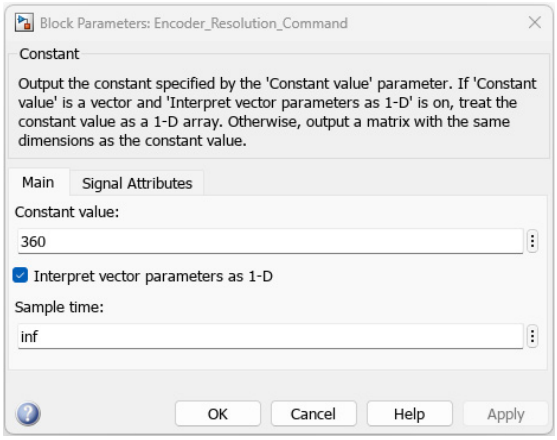

Figure 12. Encoder_Resolution_Command block window

The effect of vibrations was further monitored through the *VB_Excitation_Signal* and *VB_Transmission_Path* blocks, enabling insight into the mechanical excitation and its transmission. The effective angular disturbance resulting from vibrations was formed within

Vibration_Influence, where the input components *X* and *Y* yielded the output signal *deltatetaVibracija*, repre–senting a measurement-relevant angular deviation.

Following the definition of the vibration-induced angular disturbance, the simulation was executed by initiating the Run command to verify the correct operation of the developed model. This action launched the Mechanics Explorer window, which enabled visualisation of the simulated mechanical behaviour and provided real-time insight into the dynamic response of the system throughout the simulation interval.

3.5 Simulation of the Developed Model

Within this environment, the resulting mechanical assembly was visualised in Fig. 13 and Fig. 14. The figures presented a three-dimensional depiction of the simulated system, obtained through the import of the CAD model and its integration within the MATLAB & Simulink simulation framework.

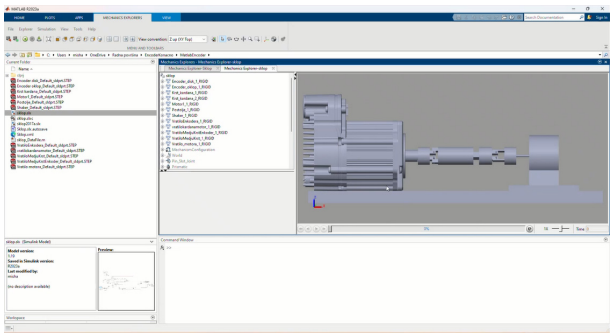

Figure 13. Simulation Overview

The visualised model described the complete mec–hanical chain, comprising the drive unit, the mechanical coupling, and the optical rotary encoder, assembled according to the defined kinematic constraints and joint configurations. Each component was treated as a rigid body, while the relative motion between elements was governed by the corresponding joints and constraint definitions established during model setup. This for–mulation enabled direct correspondence between the physical structure of the system and its functional simulation counterpart.

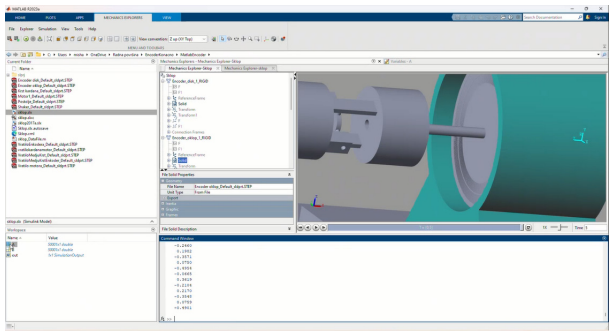

Figure 14. Representation of the Encoder in the Simulation

The Mechanics Explorer operated in synchronisation with the numerical solver, providing real-time visua–lisation of the system's kinematic behaviour during simulation execution. Although the visual output did not serve as a source of quantitative data, it played a critical role in verifying the correctness of the mechanical configuration, joint alignment, and motion consistency under dynamic operating conditions. Potential model–ling inconsistencies, such as unintended degrees of freedom or constraint conflicts, could thus be readily identified and corrected.

The numerical solution of the governing equations of motion was carried out in the time domain using an app–ropriate integration scheme, allowing continuous tracking of the system state throughout the simulation interval. The dynamic response of the system was evaluated through time-dependent signals generated within the block-diagram framework, while the Mechanics Explorer provided complementary qualitative insight into the physical plausibility of the simulated motion.

Overall, the visualised simulation model constituted a validated virtual representation of the experimental setup, supporting both structural verification and dyna–mic analysis. This integrated visual–numerical approach established a reliable basis for subsequent investigation of encoder behaviour under controlled excitation conditions and for systematic assessment of vibration-induced measurement deviations.

4. RESULTS AND DISCUSSION

4.1 Results

Based on the specified input parameters defined within the block-diagram model, the performed simulation produced a set of results that can be directly examined within the simulation environment. For the input confi–guration illustrated in Fig. 7—corresponding to an optical rotary encoder rotational speed of 100 RPM, a simulation duration of 10 s, a vibration frequency of 100 Hz, a vibration amplitude of 0.00001, and an encoder resolution of 360 PPR—the obtained results are pre–sented and discussed in the following.

The simulation yielded reference and measured angular signals that were available in a consistent form suitable for direct comparison in the angular domain. As part of the obtained results, angular quantities were expressed in degrees and aligned with discrete-time operation, enabling a uniform representation of both signals.

Consequently, the outputs REFERENCE ANGU–LAR POSITION (deg) and MEASURED ANGULAR POSITION (deg) were obtained and visualised via the Reference_Position and Measured_Position blocks. Their corresponding time-domain responses are pre–sented in Fig. 15 and Fig. 16, respectively.

These responses illustrate the temporal evolution of the reference and measured angular positions under the specified operating conditions, thereby providing a clear basis for evaluating the deviations between the two signals.

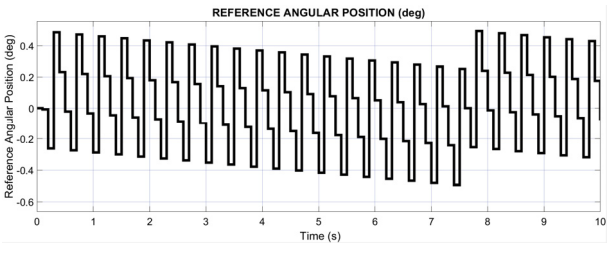

Figure 15. Reference_Position block window

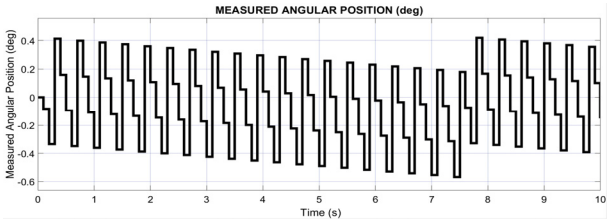

Figure 16. Measured_Position block window

The measurement error was formed using the Sub–tract block, where the difference between the reference and measured angular positions was treated as the signal delta_e_deg. Following additional alignment in Output_ Sampling, this signal was displayed via Measurement _Error as ANGULAR POSITION MEASUREMENT ERROR (deg), thereby enabling visual analysis of the temporal evolution of the measurement error (Fig. 17).

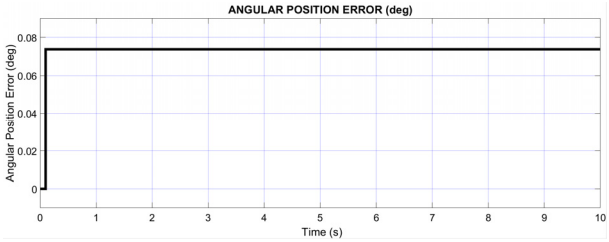

Figure 17. Measurement_Error block window

In addition to the graphical representation, a numerical presentation of the measurement error results was also provided within the block-diagram framework (Fig. 7) to enable a more detailed and quantitative inter–pretation of the optical rotary encoder performance. These numerical indicators complemented the time-domain plots and allowed direct assessment of both the magnitude and stability of the measurement error under the considered operating conditions.

The overall accuracy of the measurement was pri–marily assessed using the root mean square error, RMSE (deg), which reflects the energy content of the error signal and is therefore particularly sensitive to larger deviations. In the analysed case, the obtained value RMSE = 0.07368 deg indicated that the measurement error remained at a relatively low level throughout the simulation, confirming good global accuracy of the encoder despite the presence of vibrational excitation.

To characterise the typical magnitude of the devi–ation without overemphasising isolated extreme values, the mean absolute error, MAE (deg), was considered. The value MAE = 0.07368 deg demonstrated that the average absolute deviation closely matched the RMSE, indicating a stable and well-behaved error profile without sporadic peaks or irregular disturbances.

The presence of a systematic component in the mea–surement error was examined through the Bias (deg) metric, which captures the mean offset of the error signal over time. In this analysis, Bias = 0.07368 deg revealed a small but consistent offset, suggesting a steady systematic deviation that may be attributed to mechanical transmission asymmetries, assembly tole–rances, or a static offset in the encoder electronics rather than to random effects.

The temporal stability of the measurement was further evaluated using the standard deviation, Std (deg), which quantifies the dispersion of the error around its mean value. The obtained result Std = 0 deg indicated that the error exhibited virtually no variability over time, confirming highly repeatable behaviour and the absence of random fluctuations of significant amplitude during the simulation interval.

From a worst-case perspective, the maximum abso–lute error, Max|e| (deg), was analysed to determine the largest deviation observed irrespective of sign. The value Max|e| = 0.07368 deg demonstrated that even under the most unfavourable conditions, the deviation remained tightly bounded, which is particularly important for applications subject to strict accuracy tolerances.

The range of error variation was further charac–terised by the maximum and minimum error values, Max e (deg) and Min e (deg). In the present case, the identical values of these limits indicated symmetric and non-oscillatory error behaviour, suggesting that the deviation did not alternate between positive and negative extremes.

This observation was reinforced by the peak-to-peak error, P2P (deg), which represents the total excursion of the error signal and is sensitive to oscillatory dynamics. The value P2P = 0 deg directly confirmed the absence of periodic or vibration-induced oscillations of appre–ciable amplitude in the measurement error.

Compliance with predefined accuracy limits was assessed using the Threshold_Analysis block, which quantifies both the duration and the relative proportion of time during which the error exceeds a specified threshold of 0.5 deg. The resulting values T_thr = 0 s and R_thr = 0 % demonstrated that the measurement error remained entirely within acceptable bounds throughout the simulation, indicating robust system behaviour under the applied excitation.

The long-term tendency of the error was evaluated using the Drift_Trend analysis, where the drift rate Drift (deg/s) represents the linear evolution of the error over time. The extremely small value Drift = 1.569 × 10□□ deg/s indicated negligible long-term degradation, con–firming that no cumulative error growth occurred during the simulation interval.

The spectral characteristics of the measurement error were examined through frequency-domain analysis, with the peak frequency f_peak (Hz) identifying the dominant spectral component. The obtained value f_peak = 1.6 Hz suggested that the error was primarily associated with low-frequency dynamic excitations, typically linked to mechanical vibrations rather than high-frequency encoder noise.

Finally, the sensitivity of the measurement error to variations in system parameters was quantified using the Sensitivity Index (SI). The obtained value SI = 0.1417 indicated moderate sensitivity of the error to vibration-related dynamic parameters, confirming that mechanical vibrations exert a noticeable but not dominant influence on angular measurement accuracy.

5. DISCUSSION

The developed simulation model represents an integ–rated analytical framework that encompasses the mec–hanical, optical, and electronic parameters relevant to

the operation of optical rotary encoders. Such integration enables precise and systematic quantitative analysis of angular measurement error under a wide range of dynamic operating conditions, including variations in rotational speed and vibration parameters. The model is clearly structured, functionally coherent, and numerically stable, providing high accuracy and reproducibility of results. Consequently, the proposed simulation approach constitutes an advanced methodological basis that combines the strengths of analytical modelling and numerical simulation, enabling reliable and practically applicable analysis of measurement errors under conditions relevant to modern industrial systems.

One of the most significant aspects of this research lies in the systematic analysis of the results obtained through the developed simulation model, as well as in their internal consistency, stability, and predictability under variation of input parameters. The obtained results indicate high numerical stability of the model, with the observed deviations remaining within the expected tolerances arising from the mathematical formulation and the selected numerical methods. Such consistency supports the conclusion that the simulation model accurately represents the dynamic behaviour of the system and may be regarded as a methodologically and engineering-wise valid tool for measurement error analysis. Its formal structure, based on clearly defined mathematical relations and controlled input quantities, enables reliable interpretation of the results and confirms the conceptual validity of the proposed approach.

The strengths of the present study stem from the fully integrated simulation framework, which provides a coherent, reproducible, and analytically closed environment for quantitative assessment of the accuracy of optical rotary encoders under vibrations. The developed model enables systematic investigation of the influence of individual parameters, such as rotational speed, vibration frequency and amplitude, encoder resolution, and simulation time settings, with results obtained at a high level of repeatability and analytical clarity. This positions the simulation model as a valid and efficient alternative to conventional approaches, particularly in cases where direct experimental investigation is technically complex, financially demanding, or methodologically constrained.

An additional advantage of the developed simulation model lies in its flexibility with respect to the definition and variation of input parameters. The model allows systematic introduction of different combinations of operating conditions, yielding a range of output parameters that describe angular behaviour and measurement errors. In this manner, multiple scenarios can be analysed within the same simulation structure without the need for structural modification. This parametric approach facilitates sensitivity analysis, identification of critical operating regimes, and comparative evaluation of results, with the model functioning as a universal platform for scenario-based analysis of dynamic states.

The potential for further application of the simulation model is considerable, particularly within the field of mechanical engineering, where reliable prediction of measurement errors is a key prerequisite for system stability and optimisation. In the design and optimisation of CNC machines, the model enables rapid and accurate simulation of expected measurement errors under different operating regimes, thereby providing a solid analytical foundation for engineering decision-making already in the early stages of system design. In this way, the simulation-based approach contributes to risk reduction and increased efficiency of manufacturing processes.

The broad applicability of the proposed simulation model is also evident in industrial automated systems, robotics, and related engineering technologies, where system stability, reliability, and safety depend on accurate prediction of dynamic behaviour. Owing to its ability to deliver reproducible results under systematic variation of input parameters, the model is well suited for sensitivity analysis, development and testing of control algorithms, and simulation of systems exposed to complex dynamic loads. As such, the simulation model represents a powerful tool for virtual testing and optimisation of engineering systems.

The scientific and engineering value of this research is further reflected in the development of a unified simulation framework that combines mathematical rigour, numerical stability, and practical applicability. This approach provides a solid foundation for future research aimed at advancing simulation techniques and developing more sophisticated models for measurement error analysis. Of particular importance is the scalability of the model, which allows its extension and adaptation in accordance with technical requirements and specific industrial applications.

In a broader context, implementation of such a simulation-based approach offers substantial practical value through improved prediction and analysis of encoder errors under vibrational conditions. By enabling analytical evaluation already at the modelling stage, the approach creates opportunities for enhancing accuracy, reliability, and efficiency of mechanical systems, with direct implications for productivity and quality in industrial processes.

The perspectives for future research within the proposed simulation framework are multifaceted. One direction involves the integration of advanced optimisation algorithms and adaptive modelling techniques to enable automated adjustment of the simulation model under varying operating conditions. Another direction concerns the development of multiphysics simulation models that integrate mechanical, thermal, and electromagnetic effects, thereby achieving increased realism and analytical depth. In addition, application of the simulation concept may be extended to other types of encoders and sensor systems, significantly enhancing its generality.

In conclusion, this research represents a substantial contribution to the development of an advanced simulation model for analysing the accuracy of optical rotary encoders under vibrations. Through a systematic, mathematically grounded, and reproducible approach, the proposed model offers an innovative and practically applicable methodology with high engineering and industrial relevance, opening new opportunities for advancement in modern engineering and simulation-orientated industrial automation.

6. CONCLUSION

This study presents and details the development process of an innovative simulation-based model designed for analysing the accuracy of optical rotary encoders. The model establishes a structured and integrated platform that captures dynamic interactions and measurement deviations, enabling systematic evaluation of the effects of varying operational conditions on encoder performance.

The development of the CAD model in SolidWorks provides a precise definition of the spatial arrangement, interconnections, and mechanical logic of individual system components. This model forms a necessary foundation, establishing the structural framework upon which the simulation model is constructed. Full implementation is achieved by importing the digital model into MATLAB & Simulink and converting it into a corresponding block diagram, in which geometric arrangements are represented through functional relations and dynamic signals.

Within the resulting simulation model, variable parameters such as vibration characteristics and rotational speed are introduced and controlled, representing key factors that influence measurement errors in optical rotary encoders. Through the clearly defined block diagram structure, these parameters are linked, establishing a transparent relationship between input variables and corresponding outputs.

The model enables the generation of numerical results for encoder measurement error and provides graphical representations, rendering the simulation outcomes clear, interpretable, and suitable for further analysis.

In conclusion, the developed simulation model offers a consistent, systematic, and methodologically validated tool for investigating encoder accuracy under dynamic conditions. Its novel approach provides a foundation for future improvements, including the integration of additional environmental factors, refinement of encoder models, and adaptation to other precision electromechanical systems. The framework supports practical applications in design verification, predictive error assessment, and optimisation of high-precision measurement processes, thereby demonstrating the relevance, novelty, and utility of the model in engineering practice.

REFERENCES

[1] Crespo, D., Alonso, J., Morlanes, T. and Bernabeu, E.: Optical encoder based on the Lau effect, Opt. Eng., Vol. 39, No. 3, pp. 817–824, 2000.

[2] Sanchez-Brea, L.M. and Morlanes, T.: Metrological errors in optical encoders, Meas. Sci. Technol., Vol. 19, No. 11, 115104, 2008.

[3] Phan, X.T. and Dang, A.D.: Design and Develop a Robot Arm to Automatically Feed Workpieces for Laser Engraving Machines, FME Trans., Vol. 52, No. 4, pp. 671–680, 2024.

[4] https://etching-meltec.com/optical-encoder/

[5] Liang, L., Wan, Q., Qi, L., He, J., Du, Y., Lu, X.: The design of composite optical encoder, in: *Proceedings of the 9th International Conference on Electronic Measurement & Instruments*, 23–26.08.2009, Beijing, China, Paper 5274473.

[6] Platt, C. (with Jansson, F.): *Encyclopedia of Electronic Components*, Vol. 2, Maker Media, Sebastopol, 2015.

[7] Mayer, V. et al.: New High Resolution Optical Incremental Rotary Encoder, in: *Proceedings of the 2nd European Conference & Exhibition on Integration Issues of Miniaturized Systems - MOMS, MOEMS, ICS and Electronic Components*, 2008, pp. 1-8.

[8] Li, X., Wang, H., Kai, N., Zhou, Q., Mao, X., Zeng, L., Wang, X., Xiao, X.: Two-probe optical encoder for absolute positioning of precision stages by using an improved scale grating, Opt. Express, Vol. 24, No. 19, pp. 21378–21391, 2016.

[9] Alejandre, I., Artés, M.: Machine tool errors caused by optical linear encoders, Proc. Inst. Mech. Eng. Part B, J. Eng. Manuf., Vol. 218, No. 1, pp. 113–122, 2004.

[10] de Silva, C. W.: *Encyclopedia of Physical Science and Technology*, 3rd Ed., Elsevier, Canada, 2003.

[11] Rodriguez-Donate, C., Osornio-Rios, R., Rivera-Guillen, J. and Romero-Troncoso, R.: Fused smart sensor network for multi-axis forward kinematics estimation in industrial robots, Sensors, Vol. 11, No. 4, pp. 4104–4122, 2011.

[12] Rusiński, E., Moczko, P., Odyjas, P., Pietrusiak, D.: Investigations of structural vibrations problems of high performance machines, FME Trans., Vol. 41, No. 4, pp. 305–310, 2013.

[13] Fuchs, M., Habersohn, C., Kalkan, Y., Lechner, C. and Bleicher, F.: Metrological investigation of an actuator device for vibration assisted turning, FME Trans., Vol. 43, No. 2, pp. 119–122, 2015.

[14] Sousa, S., Nunes, E., Lopes, I.: Measuring and Managing Operational Risk in Industrial Processes, FME Transactions, Vol. 43, pp. 295–302, 2015.

[15] Phuong, L.H., Trung, P.X., Quyen, P.T., Mai, T.T.T.: Development of an intelligence vision for a robot system to pick and place objects, FME Transactions, Vol. 53, No. 2, pp. 233–242, 2025.

[16] Ramesh, R., Mannan, M.A., Poo, A.-N.: Error compensation in machine tools—A review. Part II: Thermal errors, Int. J. Mach. Tools Manuf., Vol. 40, No. 9, pp. 1257–1284, 2000.

[17] https://blog.endaq.com/vibration-measurements-vibration-analysis-basics

[18] Delbressine, F., Florussen, G.H.J., Schijvenaars, L.A., Schellekens, P.H.J.: Modelling thermomechanical behaviour of multi-axis machine tools, Precis. Eng., Vol. 30, No. 1, pp. 47–53, 2006.

[19] Kim, J.-J., Jeong, Y.H.: Thermal behaviour of a machine tool equipped with linear motors, Int. J. Mach. Tools Manuf., Vol. 44, No. 7–8, pp. 749–758, 2004.

[20] Altintas, Y., Brecher, C., Weck, M. and Witt, S.: Virtual machine tool, CIRP Ann. Manuf. Technol., Vol. 54, No. 2, pp. 115–138, 2005.

[21] Alejandre, I., Artes, M.: Thermal non-linear behaviour in optical linear encoders, Int. J. Mach. Tools Manuf., Vol. 46, pp. 1319–1325, 2006.

[22] Alejandre, I., Artés, M.: Real thermal coefficient in optical linear encoders, Exp. Tech., Vol. 28, No. 4, pp. 18–22, 2004.

[23] Weck, M., Hessel, C. and Müller-Held, B.: The virtual machine tool, Production Engineering, Vol. 7, No. 2, pp. 89–94, 2000.

[24] Florussen, G.H.J., Delbressine, F., Molengraft, M.J.G., Schellekens, P.H.J.: Assessing geometrical errors of multi-axis machines by three-dimensional length measurements, Measurement, Vol. 30, No. 4, pp. 241–255, 2001.

[25] Resor, B., Trethewey, M., Maynard, K.: Compen–sation for encoder geometry and shaft speed vari–ation in time interval torsional vibration measure–ment, J. Sound Vib., Vol. 286, No. 4–5, pp. 897–920, 2005.

[26] Shiro, Y.: Patent JP2004325171, Yaskawa Electric Corporation, 2004. Available at: https://patents.google.com/patent/JP2004325171A/en.

[27] Shinichi, U.: Patent JP2004068948, Japan Steel Works, 2004. Available at: https://patents.google.com/patent/JP2004068948A/en.

[28] Alejandre, I., Artés, M.: Method for the evaluation of optical encoders' performance under vibration, Precis. Eng., Vol. 31, No. 2, pp. 114–121, 2007.

[29] EN 60068-2-6:1996. Environmental testing. Part 2: Tests. Tests Fc: Vibration (sinusoidal), European Committee for Electrotechnical Standardization (CENELEC), Brussels, 1996.

[30] Lopez, J., Artés, M., Alejandre, I.: Analysis of optical linear encoders' errors under vibration at different mounting conditions, Meas., Vol. 44, No. 8, pp. 1367–1380, 2011.

[31] Krcheva, V., Nusev, S. and Tomić, M.: Design and Development of a Model for Accuracy Assessment and Measurement Error Quantification of Optical Rotary Encoders Under Vibration, FME Trans., Vol. 53, No. 4, pp. 545–557, 2025.

РАЗВОЈ СИМУЛАЦИОНОГ МОДЕЛА ЗА АНАЛИЗУ ТАЧНОСТИ ОПТИЧКИХ РОТАЦИОНИХ ЕНКОДЕРА ПОД ДЕЈСТВОМ МЕХАНИЧКИХ ВИБРАЦИЈА

В. Крчева, С. Нусев, М. Томић

Ова студија представља развој иновативног модела заснованог на симулацији за анализу тачности оптичких ротационих енкодера изложених механичким вибрацијама. Предложени приступ успоставља дигитално контролисано окружење које симулира стварне радне услове, омогућавајући систематско испитивање динамичких ефеката на рад енкодера. Модел интегрише основне компоненте које омогућавају формирање система способног да функционише и у дигиталном симулационом окружењу и под стварним експерименталним условима са контролисаним генерисањем механичких вибрација. Симулирањем различитих радних сценарија, модел пружа детаљну карактеризацију одступања у мерењима и идентификује варијације грешке мерења испитиваног енкодера у зависности од промена улазних параметара. Добијени увиди омогућавају предиктивну процену понашања грешке мерења и систематску оцену тачности енкодера под различитим вибрационим и радним условима. Као резултат, предложени симулациони метод представља поуздан и репродуктиван алат за испитивање грешака у мерењима изазваних вибрацијама у напредним прецизним системима.